J Clust Sci (2016) 27:1953–1962
DOI 10.1007/s10876-016-1054-3

ORIGINAL PAPER

Monodisperse Mw-Pt NPs@VC as Highly Efficient and Reusable Adsorbents for Methylene Blue Removal

Hakan Sert[1,2] · Yunus Yıldız[2] · Tugba Onal Okyay[1,2] · Bahdisen Gezer[2,3] · Zeynep Dasdelen[2] · Betül Sen[2] · Fatih Sen[2]

Received: 27 June 2016 / Published online: 26 July 2016

Abstract Addressed herein, monodisperse Vulcan carbon supported Pt nanoparticles (Mw-Pt NPs@VC) have been reproducibly synthesized using the microwave assisted method and their application for methylene blue (MB) removal from aqueous solutions was investigated through the adsorption mechanism. The prepared nanomaterials were characterized by X-ray diffraction, transmission electron microscopy, high resolution transmission electron microscopy and X-ray photoelectron spectroscopy. All results show that highly crystalline and colloidally stable nanoparticles have been formed and Mw-Pt NPs@VC were found to be one of the the most active catalyst. The results showed that the Mw-Pt NPs@VC nanoparticles had remarkable MB adsorption capacity of 271.15 mg/g. The equilibrium for MB adsorption was attained in ~55 min. Moreover, Mw-Pt NPs@VC is a reusable and promising material for MB removal since it preserves 95.6 % of its initial efficiency after six successive cycles of adsorption–desorption.

Keywords Vulcan carbon · XRD · XPS · Pt nanoparticle

Hakan Sert and Yunus Yıldız have equally contributed to this work.

Electronic supplementary material The online version of this article (doi:10.1007/s10876-016-1054-3) contains supplementary material, which is available to authorized users.

✉ Hakan Sert
hakansertdr@gmail.com

✉ Fatih Sen
fatihsen1980@gmail.com

[1] Department of Chemical Engineering, Faculty of Engineering, Usak University, Usak, Turkey

[2] Sen Research Group, Department of Biochemistry, Faculty of Art and Science, Dumlupinar University, Kütahya, Turkey

[3] Department of Electrical-Electronic Engineering, Faculty of Engineering, Usak University, Usak, Turkey

Introduction

Organic dyes are being used commonly in numerous industries. For instance, paper, coating, textile, plastic, paint, leather, and cosmetic industries produce high amounts of wastewater containing organic dyes. Those dyes are not only visible and cause esthetic problems [1, 2], but they are also highly toxic [3, 4]. In the last decades, physical, chemical and biological dye removal techniques have been used to solve this problem [5]. However, today, different techniques are being utilized to remove organic dyes from wastewaters. Those techniques include adsorption, flocculation, oxidation, biological treatment, sonochemical degradation, ultrafiltration, electrochemical degradation, and photocatalytic degradation [3, 5, 6]. When those techniques are compared, adsorption seems to be the most suitable method to remove dyes due to its high activity, practical use, and cost [2, 4, 7]. Related to this, many approaches have been performed to produce efficient adsorbents, such as activated carbon, peat, chitin, chitosan, clay materials, solid waste and silica [8, 9].

In some cases, researchers revealed those adsorbents' disadvantages like high production and treatment costs, lower adsorption capacity and efficiency, recycling and reusing problems, extended process time, and lack of specificity [2, 4, 9]. Therefore, more effective adsorbents are needed for better dye removal. In addition, even this technique performs well, dyes sometimes cannot be successfully decolorized and hence, not only new adsorbents but also novel, simple, and efficient technologies should be developed. Recently, nano-sized materials have been reported as effective and reusable adsorbents and researchers have produced and/or modified different nanomaterials for the remediation of dyes from aqueous solutions. These nanoadsorbents are mechanically flexible, chemically stable, their pore sizes are easily adjustable, and they have better structure types and ability to develop diverse compositions.

Moreover, they have large surface area which allows better contact and dye removal properties creating ideal characteristics for excellent adsorbents [10]. For example, researchers have developed polyurethane foams, polyaniline nanotubes, polypyrrole/TiO_2 nanocomposites, fullerenes, PZS nanospheres, carbon nanotubes and carbon supported nanoparticles, iron oxide nanocomposites, graphene and graphene oxide based nanocomposites and their modified types have been used for their promising dye removal properties [2, 9–11].

Besides, in literature, Pt nanoparticles are well known due to their good catalyst properties and used widely in many reactions, such as redox reactions, methanol oxidation, etc. Additionally, carbon based materials like vulcan carbon (VC), carbon blacks and fullerenes having high surface area are commonly used as catalyst supports [12–16]. Using a carbon support (such as VC), Pt nanoparticles can be deposited and nanoparticles are made more economic and utilizable [12–14].

The research for higher performing nanocomposites for dye removal requires not only the importance of adsorbent preparation strategy but also adsorbent composition [17]. Therefore, we present here Mw-Pt NPs@VC nanoparticles having significant adsorption capacity and explore their dye removal properties. Herein, we reported for the first time the synthesis of Mw-Pt NPs@VC nanoparticles via microwave assisted

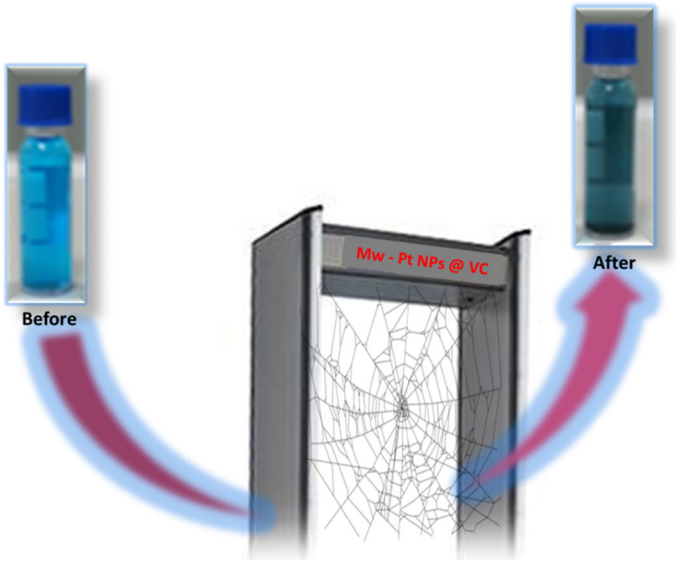

Scheme 1 The general mechanism of methylene *blue* removal in the presence of Mw-Pt NPs@VC

method for dye removal reaction (Scheme 1). The synthesized nanoparticles were characterized using X-ray diffraction (XRD), transmission electron microscopy (TEM), high resolution transmission electron microscopy (HRTEM) and X-ray photoelectron spectroscopy (XPS). Methylene blue (MB) was used as a model dye to show the applicability of Mw-Pt NPs@VC as a promising adsorbent material for organic dye removal as MB is one of the most commonly used dyes for colorizing silk, wood, and cotton. The efficiency of Mw-Pt NPs@VC nanoparticles for MB removal was studied by a UV–Vis spectrophotometer. The effect of contact time, the relationship between the amounts of Mw-Pt NPs@VC adsorbed per unit weight of MB, and the reusability were studied. It was indicated that this new type of adsorbent has higher surface area, easy and rapid extraction/regeneration, ease of operation, and potential use for wastewater remediation studies.

Materials and Methods

Preparation of Mw-Pt NPs@VC

To form a stable suspension, 0.25 mmol $PtCl_4$ was dispersed in 30 mL of ethylene glycol solution under vigorous stirring. Next, pH was adjusted to 12 using a NaOH–EG solution. Then, this solution was put in the central point of a microwave oven (1200 W) for consecutive heating time of 60 s. Under this environmental condition, EG acts as the reducing agent for $PtCl_4$ reduction. After, filtration of the product was performed and then washing steps were done using acetone and deionized water for several times. Mw synthesis was performed with oleylamine, which was used as a

capping agent for the starting materials, for stabilizing the metal nanoparticles against agglomeration. Employing an ultrasonic tip sonicator, the prepared NPs were mixed with VC having a 1:1 ratio. Finally, using a vacuum-drier at room temperature, the Mw-Pt NPs@VC NPs were dried.

Results and Discussion

XRD, TEM, HRTEM and XPS, have been utilized to characterize the monodisperse Mw-Pt NPs@VC. The XRD data seen in Fig. 1 showed distinct diffraction patterns of monodisperse Mw-Pt NPs@VC. In XRD pattern, Pt (111), (200), (220) and (311) planes of the face-centered cubic crystal lattice of Pt were observed as diffraction peaks at $2\theta = 39.87°$, 46.21°, 67.67° and 81.47° (JCPDS-ICDD, card no. 04-802), which points out that Mw-Pt NPs@VC is in the face-centered cubic crystalline structure. It was shown that monodisperse Mw-Pt NPs@VC had a lattice parameter value of 3.921 Å. To do this, the following equation was used by the help of Pt (220) diffraction peak of prepared catalyst which is in agreement with 3.923 Å for pure Pt [18–26];

$$Sin\,\theta = \frac{\lambda\sqrt{h^2 + k^2 + l^2}}{2a}$$

(for a cubic structure).

Furthermore, using the Debye–Scherrer equation [27–37], average crystallite Pt particle size of monodisperse Mw-Pt NPs@VC was calculated as 4.36 ± 0.44 nm.

The particle size and the distribution of the Mw-Pt NPs@VC were analyzed using HRTEM (Fig. 2a). The approximate particle size was found as 4.28 ± 0.45 nm (Fig. 2b). It was observed that the particles were mostly spherical, and besides, there was not any agglomeration.

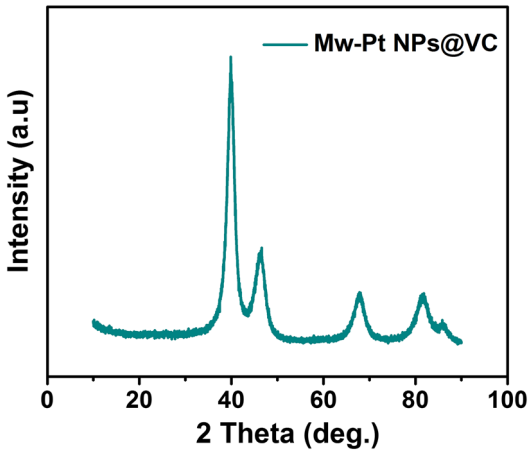

Fig. 1 XRD pattern of Mw-Pt NPs@VC

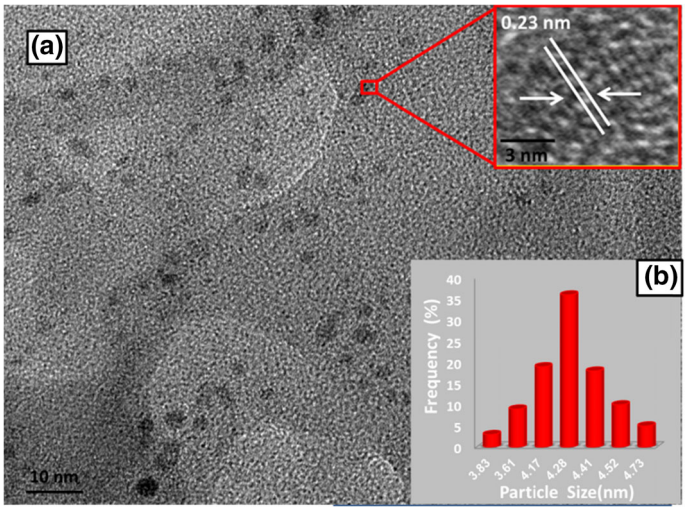

Fig. 2 **a** TEM-HRTEM image and **b** particle size *histogram* of Mw-Pt NPs@VC

Furthermore, for Mw-Pt NPs@VC, the representative atomic lattice fringes were also depicted in Fig. 1b. It was found that, on the prepared catalyst, Pt (111) plane spacing is 0.23 nm, and this is exactly same with nominal Pt (111) spacing of 0.23 nm.

In addition, for investigation of adsorbent surface contents and the oxidation state of Pt in the monodisperse Mw-Pt NPs@VC, XPS was utilized. Thus, the spectrum's Pt 4f region was evaluated. By employing the Gaussian–Lorentzian method, XPS peak was fit. After smoothing and subtracting the Shirley-shaped background, each peak's integral was counted to estimate the related strength of the species. By referencing to the C 1s peak at 284.6 eV, accurate binding energies (±0.3 eV) were examined in XPS spectrum results.

In Fig. 3, the Pt 4f photoelectron spectrum of the monodisperse Mw-Pt NPs@VC comprising two pairs of doublet was shown. At about 70.9 and 74.2 eV, which are the most intense doublets, a signature of metallic Pt was indicated [38–43]. The other doublets at about 72.1–75.4 and 74.4–77.7 eV are presumably led by an extremely little proportion of oxidized or unreduced Pt species while the catalyst contacting with the air. Since Pt(0)/Pt(II)+(IV) proportion for the synthesized catalyst was computed as 3.24, the prepared catalyst are mostly in zero oxidation state.

Having sufficiently characterized the monodisperse Mw-Pt NPs@VC, we turned our attention on exploiting their utility in the dye removal reaction. In this frame, it is worth mentioning that Pt NPs is often used as a catalyst in alcohol oxidation, dehydrogenation and/or hydrolysis reactions [21–45] but its use as an adsorbent for the MB removal from aqueous solutions has not been reported before. Furthermore, the usage of microwave assisted method in current work may be regarded as a rapid, appropriate, attractive, useful, simple and one of the safest procedures for the synthesis of an effective heterogeneous nanoadsorbent system.

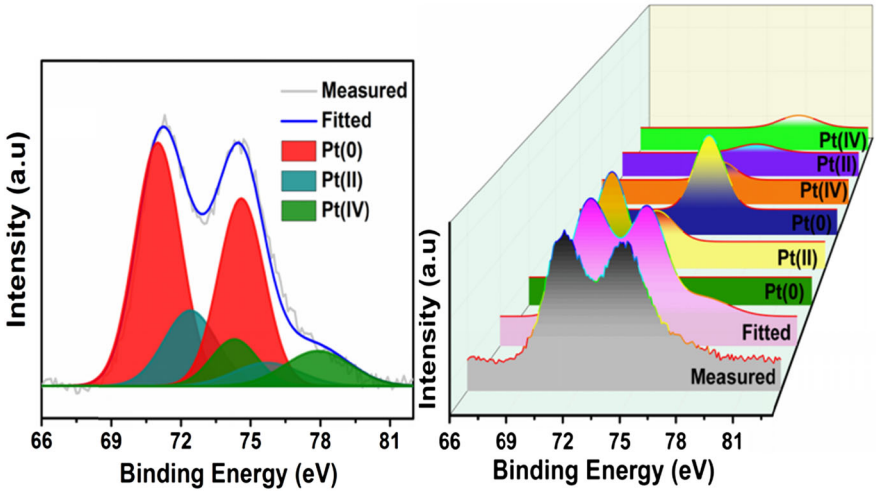

Fig. 3 XPS spectra of Pt 4f region

The adsorption property of the Mw-Pt NPs@VC synthesized was examined to remove MB from water. To do that, firstly, a calibration curve was prepared for the MB solutions which had different concentrations (2.5, 5, 10, 20, and 30 mg/L) (Fig. S1). Next, how dye adsorption is influenced by the contact time at room

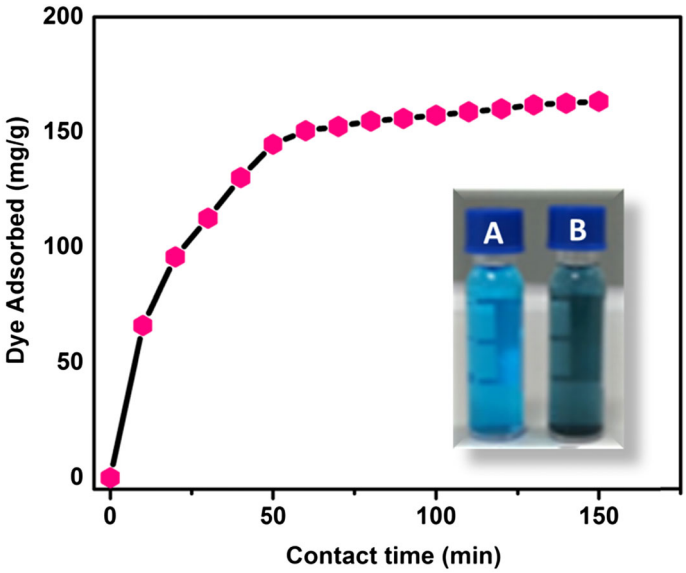

Fig. 4 Change of adsorption capacity of Mw-Pt NPs@VC nanoparticles at different contact time. The initial concentration of MB was 13 mg/L. The two tubes are the representative images for MB solutions before dye adsorption (**a**) and after dye adsorption (**b**)

temperature was studied and its results were given in Fig. 4. In these experiments, aqueous MB solutions (13 mg/L) were used and contact time effect on the adsorption activity of the Mw-Pt NPs@VC nanocomposites was determined. At high MB concentrations, some dye aggregation was observed. The results showed that MB adsorption by the Mw-Pt NPs@VC nanocomposites reached equilibrium after 60 min. This equilibrium time can be considered short and hence, it can be stated that Mw-Pt NPs@VC nanocomposites possess high adsorption efficacy for MB removal.

Moreover, in the beginning of the contact time experiments, it was also seen that the MB removing efficiency of Mw-Pt NPs@VC nanocomposites was fast, but afterwards it became slower. The reason for this is the decrement in the MB concentration; as MB concentration decreases during the adsorption process, the speed of adsorption slows down.

In Fig. 5 the adsorption isotherm was displayed and the correlation (at equilibrium) between the amounts of Mw-Pt NPs@VC adsorbed per unit weight of the MB dye (q_e, mg/g) and the concentrations of dye in the solution (C_e, mg/L) was presented. The maximum adsorption capacity was calculated as 271.15 mg/g. When this is compared to other adsorbents reported previously in the literature, this

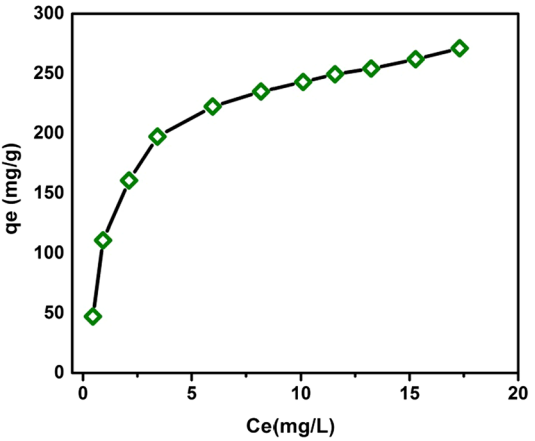

Fig. 5 Adsorption isotherm of Mw-Pt NPs@VC nanoparticles for MB removal

Table 1 The adsorption capacity of various materials tested in MB removal

Adsorbent	Adsorption capacity (mg MB/g)	Reference
Mw-Pt NPs@VC	271.15	Our Study
MPB-AC	163.3	[44]
PZS nanospheres	20	[2]
GO–Fe_3O_4 hybrids	172.6	[1]
MWCNTs with	42.3	[45]
Na-ghassoulite	135	[46]
Mw-Pt NPs	167.27	Our Study
VC	110.24	Our study

catalyst has one of the highest adsorption capacities (Table 1). BET results indicate that the specific surface areas of Mw-Pt NPs@VC and Mw-Pt NPs are 112.6 and 46 m^2/g, respectively. These results prove that VC support cause the increase in adsorbent capability of Pt nanoparticles.

As the nanocomposites' stability is very important for easy and practical applications as adsorbents for wastewater treatment, the stability of Mw-Pt NPs@VC nanoparticles was examined in this study. Results showed that not much changes occured in the structure of Mw-Pt NPs@VC after MB adsorption (Fig. 6a). This indicated the stability of the Mw-Pt NPs@VC nanoparticles in aqueous

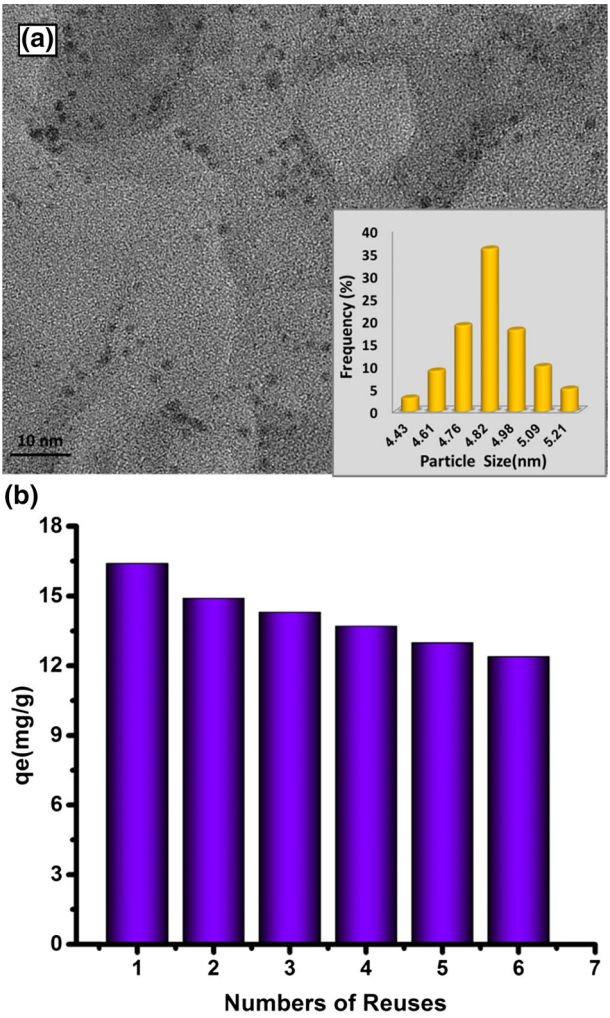

Fig. 6 **a** A representative TEM image of the Mw-Pt NPs@VC nanocomposite after MB adsorption; **b** The reusability of the Mw-Pt NPs@VC nanocomposite for MB removal performed for 6 successive cycles. ([Mw-Pt NPs@VC] = 0.25 g/L; [MB] = 13 mg/L; T = 25 °C; contact time = 30 min)

solutions. Furthermore, as good adsorbents have to possess high adsorption capacity and desorption property for its practical use, the reusability needs to be evaluated [46, 47]. Hence, in this study, Mw-Pt NPs@VC nanoparticles were tested for their reusability. To do that, 6 cycles of adsorption–desorption were perfomed as shown in Fig. 6b. It can be seen from the results that the adsorption capacity of Mw-Pt NPs@VC nanoparticles for MB removal decreased a little after each adsorption–desorption cycle; but Mw-Pt NPs@VC still showed 95.6 % of the initial efficiency after 6 cycles.

Our results revealed that the regenerated Mw-Pt NPs@VC nanoparticles can be used repeatedly as an efficient adsorbent for MB removal (Fig. 6b). Based on our results, the Mw-Pt NPs@VC nanoparticles are highly efficient for MB removal, have reusability with high adsorption capacity and adsorption rate.

Conclusions

In the present study, a simple, ecofriendly and effective method was presented to produce Mw-Pt NPs@VC nanoparticles successfully. The results exhibited we had very short reaction times, great yields, simple methodology and significant MB removal capacity (271.15 mg MB/g Mw-Pt NPs@VC) most likely owing to monodispersity of Mw-Pt NPs@VC, high specific surface area and % metal substance of Mw-Pt NPs@VC. In addition, good stability and potential for reusability of the absorbent were observed.

It was found out that 95.6 % of the initial capacity remains after six adsorption–desorption cycles were performed. These Mw-Pt NPs@VC nanoparticles have great potential applications for removing organic dyes from polluted waters.

Acknowledgments This research was financed by the Dumlupınar University Research Fund (Grant No. 2014-05, 2015-35 and 2015-50). The partial supports by Science Academy and Fevzi Akkaya Research Funding (FABED) are gratefully acknowledged.

References

1. K. Meral and Ö. Metin (2014). *Turk. J. Chem.* **38**, 775–782.
2. Z. Chen, J. Fu, M. Wang, X. Wang, J. Zhang, Q. Xu, and R. A. Lemons (2014). *Appl. Surf. Sci.* **289**, 495–501.
3. B. Yu, X. Zhang, J. Xie, R. Wu, X. Liu, H. Li, F. Chen, H. Yang, Z. Ming, and S.-T. Yang (2015). *Appl. Surf. Sci.* **351**, 765–771.
4. G. Crini (2006). *Bioresour. Technol.* **97**, 1061–1085.
5. M. Rafatullah, O. Sulaiman, R. Hashim, and A. Ahmad (2010). *J. Hazard. Mater.* **177**, 70–80.
6. F. Liu, H. Zou, J. Hu, H. Liu, J. Peng, Y. Chen, F. Lu, and Y. Huo (2016). *Chem. Eng. J.* **287**, 410–418.
7. M. A. Khan, S.-H. Lee, S. Kang, K.-J. Paeng, G. Lee, S.-E. Oh, and B.-H. Jeon (2011). *Sep. Sci. Technol.* **46**, 1121–1130.
8. M. S. Chiou, P. Y. Ho, and H. Y. Li (2004). *Dyes Pigments* **60**, 69–84.
9. L. Bai, Z. Li, Y. Zhang, T. Wang, R. Lu, W. Zhou, H. Gao, and S. Zhang (2015). *Chem. Eng. J.* **279**, 757–766.
10. L. Fan, C. Luo, M. Sun, H. Qiu, and X. Li (2013). *Coll. Surf. B Biointerfaces* **103**, 601–607.

11. F. Liu, S. Chung, G. Oh, and T. S. Seo (2012). *ACS Appl. Mater. Interfaces* **4**, 922–927.
12. X. Li, F. Feng, K. Zhang, S. Ye, D. Y. Kwok, and V. Birss (2012). *Langmuir* **28**, 6698–6705.
13. V. Malgras, H. A. Esfahani, H. Wang, B. Jiang, C. Li, K. C.-W. Wu, J. H. Kim, and Y. Yamauchi (2015). *Adv. Mater.* **28**, 993–1010.
14. C. Li and Y. Yamauchi (2013). *Phys. Chem. Chem. Phys.* **15**, 3490–3496.
15. Y. Li, B. P. Bastakoti, V. Malgras, C. Li, J. Tang, J. Ho Kim, and Y. Yamauchi (2015). *Angew Chem. Int. Ed.* **54**, 11073–11077.
16. J. T. Moore, J. D. Corn, D. Chu, R. Jiang, D. L. Boxall, E. A. Kenik, and C. M. Lukehart (2003). *Chem. Mater.* **15**, 3320–3325.
17. Y. Garsany, A. Epshteyn, A. P. Purdy, K. L. More, and K. E. Swider-Lyons (2010). *J. Phys. Chem. Lett.* **1**, 1977–1981.
18. F. Sen, Y. Karatas, M. Gulcan, and M. Zahmakiran (2014). *RSC Adv.* **4**, 1526–1531.
19. F. Sen, G. Gokagac, and S. Sen (2013). *J Nanopart. Res.* **15**, 1979.
20. J. Xu, H. Lv, S. T. Yang, and J. Luo (2013). *Inorg. Chem.* **33**, 139–160.
21. D. R. Dreyer, S. Park, C. W. Bielawski, and R. S. Ruoff (2010). *Chem. Soc. Rev.* **39**, 228–240.
22. F. Ahmed and D. F. Rodrigues (2013). *J. Hazard. Mater.* **256–257**, 33–39.
23. C. O'Neill, F. R. Hawkes, D. L. Hawkes, N. D. Lourenco, H. M. Pinheiro, and W. Delee (1999). *J. Chem. Technol. Biotechnol.* **74**, 1009–1018.
24. Z. Liu, X. Y. Ling, X. Su, and J. Y. Lee (2004). *J. Phys. Chem. B* **108**, 8234–8240.
25. B. Celik, S. Kuzu, E. Erken, H. Sert, Y. Koskun, and F. Sen (2016). *Int. J. Hydrog. Energy* **41**, 3093–3101.
26. H. Goksu, Y. Yıldız, B. Celik, M. Yazici, B. Kilbas, and F. Sen (2016). *Catal. Sci. Technol*. doi:10.1039/C5CY01462J.
27. B. Aday, Y. Yıldız, R. Ulus, S. Eris, M. Kaya, and F. Sen (2016). *New J. Chem.* **40**, 748–754.
28. B. Celik, G. Baskaya, H. Sert, O. Karatepe, E. Erken, and F. Sen (2016). *Int. J. Hydrog. Energy*. doi:10.1016/j.ijhydene.2016.02.061.
29. B. Celik, Y. Yildiz, H. Sert, E. Erken, Y. Koskun, and F. Sen (2016). *RSC Adv.* **6**, 24097–24102.
30. E. Erken, H. Pamuk, Ö. Karatepe, G. Başkaya, H. Sert, O. M. Kalfa, and F. Şen (2016). *J. Cluster Science* **27**, 9–23.
31. Y. Yıldız, H. Pamuk, Ö. Karatepe, Z. Dasdelen, and F. Sen (2016). *RSC Advances* **6**, 32858–32862.
32. E. Erken, Y. Yildiz, B. Kilbas, and F. Sen (2016). *J. Nanosci. Nanotechnol.* **16**, 5944–5950.
33. B. Çelik, E. Erken, S. Eriş, Y. Yıldız, B. Şahin, H. Pamuk, and F. Sen (2016). *Catal. Sci. Technol.* **6**, 1685–1692.
34. E. Erken, I. Esirden, M. Kaya, and F. Sen (2015). *Catal. Sci. Technol.* **5**, 4452.
35. H. Pamuk, B. Aday, F. Sen, and M. Kaya (2015). *RSC Adv.* **5**, 49295–49300.
36. F. Sen and G. Gokagac (2008). *Energy Fuels* **22**, 1858–1864.
37. Z. Ozturk, F. Sen, S. Sen, and G. Gokagac (2012). *J. Mater. Sci.* **47**, 8134–8144.
38. F. Sen, S. Sen, and G. Gokagac (2011). *Phys. Chem. Chem. Phys.* **13**, 1676–1684.
39. F. Sen and G. Gokagac (2014). *J. Appl. Electrochem.* **44**, 199–207.
40. S. Sen, F. Sen, and G. Gokagac (2011). *Phys. Chem. Chem. Phys.* **13**, 6784–6792.
41. F. Sen and G. Gokagac (2007). *J. Phys. Chem. C* **111**, 1467–1473.
42. E. Erken, I. Esirden, M. Kaya, and F. Sen (2015). *RSC Adv.* **5**, 68558–68564.
43. F. Sen and G. Gökagac (2007). *J. Phys. Chem. C* **111**, 5715–5720.
44. K. T. Wong, N. C. Eu, S. Ibrahim, H. Kim, Y. Yoon, and M. Jang (2016). *J. Clean. Prod.* **115**, 337–342.
45. S. Qu, F. Huang, S. Yu, G. Chen, and J. Kong (2008). *J. Hazard. Mater.* **160**, 643–647.
46. Y. El Mouzdahir, A. Elmchaouri, R. Mahboub, A. Gil, and S. Korili (2007). *J. Chem. Eng. Data* **52**, 1621–1625.
47. W. Yao, T. Ni, S. Chen, H. Li, and Y. Lu (2014). *Compos. Sci. Technol.* **99**, 15–22.